

# Titanium Surface Nanostructuring by Picosecond Laser Irradiation for Surface Improvement of Dental Abutments

Florin Jipa<sup>1</sup>, Paula Florian<sup>1,2</sup>, Madalina Icriverzi<sup>1,2</sup>, Gianina Popescu-Pelin<sup>1</sup>, Dragos Budei<sup>3,4</sup>, Emanuel Axente<sup>\*1</sup>, Koji Sugioka<sup>5</sup>, and Felix Sima<sup>\*1,5</sup>

<sup>1</sup>National Institute for Laser, Plasma and Radiation Physics (INFLPR), 409 Atomistilor, Magurele 077125, Romania

<sup>2</sup>Institute of Biochemistry of the Romanian Academy, 296 Splaiul Independentei, Bucharest 060031, Romania

<sup>3</sup>Dentix Millennium SRL, 087153 Giurgiu, Romania

<sup>4</sup>Applied Chemistry and Material Sciences Faculty, Inorganic Chemistry, Physics Chemistry and Electro-Chemistry Department, Polytechnic University of Bucharest, 1-7 Ghe. Polizu, Bucharest 060031, Romania

<sup>5</sup>RIKEN Center for Advanced Photonics, 2-1 Hirosawa, Wako, Saitama, 351-0198, Japan

\*Corresponding author's e-mails: [emanuel.axente@inflpr.ro](mailto:emanuel.axente@inflpr.ro), [felix.sima@inflpr.ro](mailto:felix.sima@inflpr.ro)

The goal of this study is to demonstrate the capability of high-repetition rate picosecond laser processing as an alternative approach for large-scale surface nanostructuring of Titanium (Ti) dental abutments. We used the second harmonic (532 nm) of the Nd:YVO<sub>4</sub> laser source, delivering pulses of about 10 ps duration at 500 kHz repetition rate. Sample surfaces were irradiated in air with various light doses, affecting surface morphologies in both micro- and nano-scales. Scanning electron microscopy analyses revealed the generation of laser-induced periodic surface structures (LIPSS), with feature sizes similar to the laser wavelength. We evidenced that the color of samples surface varied by changing the applied doses due to the gradual oxidation of surfaces. The influence of morphological and chemical surface features (generated by a medium irradiation dose) on viability, proliferation, adhesion and morphology of human mesenchymal stem cells (hMSCs) was evaluated at 3 and 7 days after cell seeding. Immunofluorescence microscopy investigations of the cytoskeleton have shown that all the investigated surfaces promote hMSCs adhesion. We demonstrate that picosecond laser nanostructuring of Ti metallic surfaces is able to modulate hMSCs viability and proliferation through morphological modifications to promote a better cells growth and adhesion as compared with controls after 7 days of culture.

DOI: 10.2961/jlmn.2023.03.2003

**Keywords:** laser processing, titanium nanostructuring, LIPSS, hMSCs, biocompatibility assays.

## 1. Introduction

Titanium (Ti) and its alloys are the most common materials used for the fabrication of dental and bone implants due to their excellent biocompatibility [1], mechanical properties [2], and corrosion resistance [3]. Osteoblast cell adhesion on biomaterials and the influence of surface topography and chemistry on cells behavior were largely explored in the last decades [4,5]. In case of dental implant abutments, because the surface is in contact with soft gingival tissues, it is necessary to be modified such that morphological characteristics promote optimal cell adhesion and sealing against bacterial invasion [6,7].

Surface improvement of dental implants by various functionalization approaches was extensively studied, to increase implant's life-time. The strong attachment of the mucosa to the dental abutment could limit bacterial penetration and biofilm formation at the interface, and thus, prevent peri-implant disease and finally implant failure.

Currently, there are several classical strategies for surface modification of metallic implants such as acid-etching [8], sand blasting [9], grinding [10], and plasma spraying

[11]. Novel approaches are also reported, including but not limited to synthesis of biomimetic coatings of Calcium Phosphates [12], biopolymers [13], and Extracellular Matrix Proteins [7,14].

Laser processing of Ti dental implants has shown to allow obtaining similar surface characteristics with the classical implant's modification strategies, but without any surface contaminations [15]. Indeed, laser technologies offers clean and reproducible processes enabling a high control of the experimental parameters. Other advantages are related to the possibility to obtain large specific surface area and chemistry that could influence osseointegration. A comprehensive review on laser engineering of biomimetic surfaces, covering a broad range of applications, is available in Ref. [16].

A particular feature of laser patterning is the possibility to generate laser-induced periodic surface structures (LIPSS), also known as ripples, on metals, semiconductors and dielectrics in a fast and cost-effective processing [17]. The mechanisms of ripple formation and their proposed applications were extensively addressed with the techno-

logical progress of ultrashort, high-power pulsed laser systems [18-20]. The potential applications are related to the generation of structural colors [21], tailoring the wetting behavior of the surfaces [22], antibiofouling [23], but also the possibility to fabricate surfaces with anti-bacterial adhesion properties [24]. Very recently, Sotelo *et al.* [24] have demonstrated the influence of LIPSS generated on TiAl6V4 surfaces, on cell/bacteria attachment. It has been shown that laser structured surfaces are able to improve the differentiation of human osteoblast-like MG63 cell line, while reducing bacterial activity (*S. aureus* and *E. coli*) and biofilm formation.

In this study, we propose to use high-repetition rate picosecond laser processing, as an alternative approach for large-scale surface nanostructuring of Ti for dental abutments. The influence of surface features on human mesenchymal stem cells behavior is evaluated and confirm that laser processing could improve abutment surface performances and cytocompatibility.

## 2. Materials and methods

### 2.1 Laser processing and surface characterization

The experimental setup used in this study consists of a high-repetition rate picosecond laser source (Coherent, model Lumera HyperRapid 50), delivering pulses of less than 10 ps duration, at 1064 nm and 500 kHz. Surface micro-processing was carried out using the second harmonic (532 nm) of the laser at 2.2 W power. The beam was focused onto the sample surface using an aspheric lens of 35 mm focal length to generate a circular spot of about 15  $\mu\text{m}$  in diameter.

The samples were placed on motorized translation stages (PlanarDL, Aerotech) with a spatial resolution of few tens of nanometers and scanned in a plane perpendicular to the laser incidence direction with a speed fixed at 1 mm s<sup>-1</sup> and a step between lines of 25  $\mu\text{m}$ . The experiments were carried out in a clean room in air at atmospheric pressure, and were in-situ monitored with a CCD camera. A schematic representation of the experimental setup is presented in Figure 1.

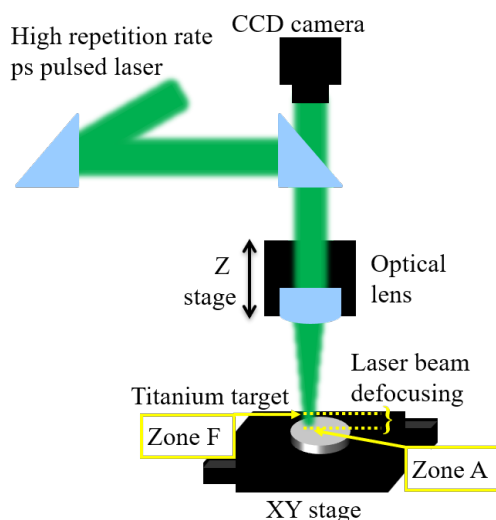


Fig. 1 Schematic representation of the experimental setup.

The morphological and compositional characterization of the samples were performed by Scanning Electron Microscopy (SEM) using an Apreo S (Thermo Fisher Scientific) microscope coupled with an Energy-dispersive X-ray spectroscopy (EDAX) Inc detector.

### 2.2 In vitro tests

#### Primary human mesenchymal stem cells

Primary hMSC were obtained from bone marrow aspirates and isolated by density gradient centrifugation, as previously described [25]. The hMSC cells were grown in complete Dulbecco's Modified Eagle Medium (DMEM) with low glucose (1 g/L), supplemented with 10% (v/v) fetal bovine serum (FBS) and 1% (v/v) streptomycin/penicillin (all from Gibco (Life Technologies, Paisley, UK)). The cells were maintained in culture at a density of  $5 \times 10^3$  cells/cm<sup>2</sup> ( $2 \times 10^3$  cells in 96-well plates), for 3 and 7 days, respectively.

#### Cell proliferation assay-direct method

Before biocompatibility investigations all materials were sterilized in a Falcon 30 Autoclave (LTE Scientific, UK) using water vapors at 121 °C and 1 atm, for 30 min, before interaction with the cells.

Proliferation of hMSC cells was evaluated by MTS ([3-(4,5-dimethylthiazol-2-yl)-5-(3-carboxymethoxyphenyl)-2-(4-sulfophenyl)-2H-tetrazolium, inner salt]) assay (CellTiter 96® Aqueous Non-Radioactive Cell Proliferation Assay, Promega, USA) according to the manufacturer's instructions. The method is based on the conversion of the tetrazolium compound (MTS) to a formazan dye by mitochondrial dehydrogenases from viable cells.

The hMSC cells were placed in 96-well cell culture plates (NUNC) at a cell density of  $2 \times 10^3$  cells /well on laser processed Ti surfaces and incubated for 3 and 7 days at 37 °C. The cells grown on Coverslip and bare Ti substrates were used as controls. The absorbance values recorded at 450 nm on a microplate reader (Mithras, Berthold Technology, Germany) were directly proportional to the number of living cells.

#### Immunofluorescence microscopy

The hMSC cultured in direct contact with all surfaces for 3 and 7 days were investigated for cytoskeleton protein distribution by immunofluorescence techniques. Cells were fixed with 4% paraformaldehyde (PFA) for 10 min, permeabilized with 0.2% Triton X-100 solution, and blocked for 1 h with 0.5% bovine serum albumin solution. Cells were labeled with primary mouse anti-human vinculin antibodies (Sigma-Aldrich, USA) for 30 min before incubation with secondary antibodies goat anti-mouse conjugated with Alexa Fluor 594 (Thermo Fisher Scientific, USA). For actin labeling, the specimens were incubated for 30 min with phalloidin reagent conjugated with Alexa Fluor 488 (Thermo Fisher Scientific). The nuclei were counterstained for 1 min with Hoechst fluorescent dye (Life Technologies, Molecular Probes, USA) and then the samples were mounted with FluorSave™ Reagent (Merck-Millipore) before microscopy visualization using a Zeiss AxioCam Erc5s fluorescence microscope with ApoTome 2 module and image acquisition was performed using AxioCam MRm camera

(10× objective). For image editing, the Axio Vision Rel 4.8 software was utilized (Zeiss, Jena, Germany).

Scanning electron microscopy observation of hMSCs cells

To investigate cellular morphology in direct contact with biomaterials surface, the hMSC were grown onto the surfaces of unprocessed Ti, laser processed Ti and Coverslip controls for 3 and 7 days and prepared for SEM imaging. Briefly, the cells were fixed with 2.5% glutaraldehyde and then dehydrated by sequential immersion in 70%, 90% and 100% ethanol. All samples were washed with 50% and 75% hexamethyldisilazane (HMDS) solution prepared in ethanol and finally in 100% HMDS. The specimens were subjected to HMDS evaporation in a Euroclone AURA 2000 M.A.C. (BioAir, Italy) fume hood. All samples were first air-dried and then metalized with a 100 Å thin silver layer, deposited using a BAL-TEC SCD 005 sputter coater (Schalksmühle, Germany). A FEI Inspect S50 (Hillsboro, OR, USA) scanning electron microscope was used.

**3. Results and Discussions**

**3.1 Morphological and compositional analyses**

In order to investigate the influence of the applied laser dose on surface characteristics, we scanned Ti surface areas of  $1 \times 1 \text{ mm}^2$ . The power was kept fixed, but the applied laser dose was changed by changing the diameter of the laser spot. Thus, the beam was defocused between 2.5 mm (Zone A) to 3.75 mm (Zone F) with respect to focus, with a step of 250 μm by decreasing the distance between the sample and the lens position using a z stage (Figure 1). Accordingly, the laser fluences applied to Ti surface was decreased from 9 to 4 mJ cm<sup>-2</sup> from Zone A to Zone F.

We observed that the color of the sample surface varied by changing the applied dose (Figure 2.a). There are three distinct physical mechanisms responsible for color change on Ti surface due to laser irradiation: laser-induced oxidation, ripples formation, and micro/nanoparticles generation [21]. The initial morphology of the untreated Ti surface is presented in Figure 2.b.

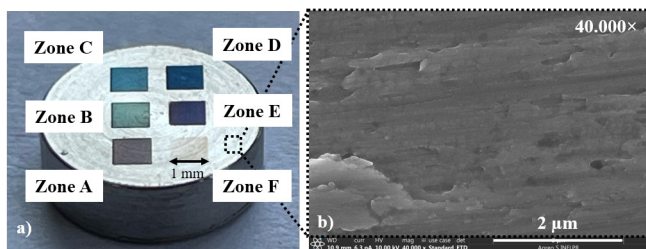


**Fig. 2** Image of the laser-treated Titanium surface with irradiation dose decrease from zone A to Zone F (a). SEM image of the unprocessed Titanium surface (b). Scale bar is 2 μm.

The generation of ripples is confirmed by SEM analyses (Figure 3). The images reveal feature sizes of hundreds of nanometers, similar to the laser wavelength but different topologies depending on the applied dose. The threshold for ripples formation was found in Zone F (Figure 2.a) while the pattern morphology changed, specifically larger structures were formed at higher laser doses (Figure 3).

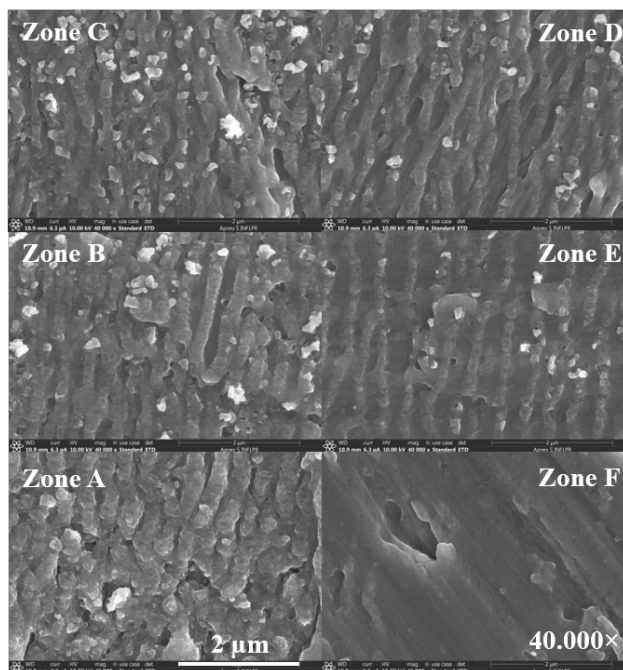


**Fig. 3** SEM images of the laser-treated Titanium surface for different irradiation doses (decrease from zone A to zone F), at 40.000× magnification. Laser polarization was perpendicular to LIPSS orientation. Scale bar is 2 μm in all images.

Energy-dispersive X-ray spectroscopy (EDXS) analyses evidenced that laser nanostructuring is a clean process. Despite Ti and the oxide layers, only a slight C contamination of about 4-5 at% was noticed on controls and laser treated samples (Figure 4). Moreover, quantitative analyses of the irradiated zones evidenced an increase of O content (up to ten times) with increasing the applied laser dose. This means that with increasing the applied laser dose, a thicker oxide layer is formed due to material reaction with oxygen catalyzed by laser local heating. Laser-induced oxidation of titanium and its alloys were reported in several studies, in which physical-chemical analyses revealed the mechanisms of surface modification [26-28]. It was shown that few hundreds of nanometers thick oxide layers or thicker, when increasing the applied laser fluence, could be obtained, as evidenced by depth profiling [26].

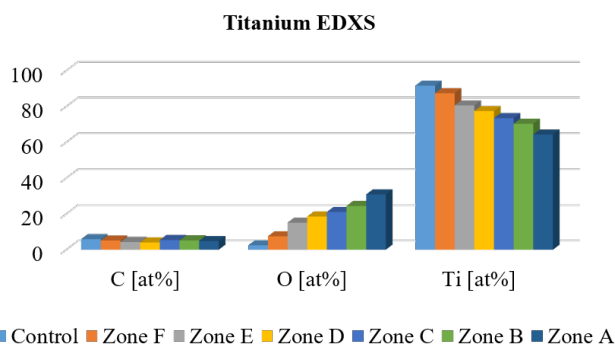


**Fig. 4** EDXS analyses of the laser-treated Titanium surface for different irradiation doses (increase from zone F to Zone A), with respect to untreated sample (control).

In the following, 14 Ti samples were laser processed by a medium laser irradiation dose (Zone C in Figure 3), in a single experimental run, to be used for the biochemical

assays. Large-scale, uniform and homogeneous structures are visible all over the surfaces (Figure 5), without cracks or other visible defects. For these structures the roughness is below 10 nm (data not shown).

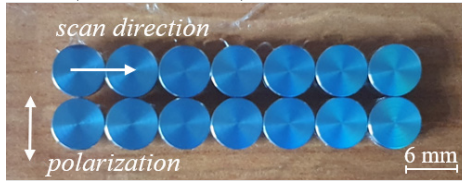


Fig. 5 Photograph of samples exposed to laser processing by a medium irradiation dose, corresponding to Zone C.

### 3.2 Biochemical assays

After laser processing, the samples were kept in closed plastic containers for 30 days in air, at room temperature and atmospheric pressure before cells seeding. All the samples were cleaned using standard protocols, as described in section 2.2.

The influence of morphological and chemical surface features on viability, proliferation, adhesion and morphology of human mesenchymal stem cells (hMSCs) was evaluated at 3 and 7 days after cell seeding.

MTS assay has shown that cell viability and proliferation at 7 days of culture in direct contact with surface materials investigated are better on laser treated samples compared to Ti control and coverslip (Figure 6).

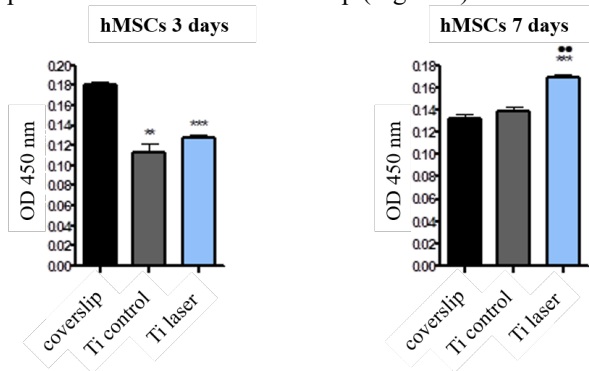


Fig. 6 hMSCs cell viability after 3 days (left) and 7 days (right) of culture on laser processed and unprocessed Ti. Values considered statistically significant \*\*  $p < 0,01$ , \*\*\*  $p < 0,001$  with respect to CTRL (cells grown on coverslip), \*\*  $p < 0,01$  with respect to unprocessed Ti (TiCP4 CTRL).

Cell adhesion is an important event that precedes the cell proliferation, and involves proteins of the cytoskeleton that strongly interact with each other, such as actin filaments, and vinculin. Vinculin is a key Focal Adhesion (FA) molecule that controls FA maturation by interactions with actin protein, and the size of focal adhesion complex is characterized by vinculin staining. Thus, the morphology and skeleton of the hMSC cells were investigated by labeling actin and vinculin, which are protein initiating the cell adhesion process, in all tested samples.

As shown in Figure 7, the actin filaments were elongated and polymerized, forming a network-like appearance sustaining the cells in the process of adhesion, in all control samples. In addition, a basket-like actin filaments distribution, with a circumferential pattern at the plasma membrane was observed in the case of laser nanostructured Ti surfaces (Figure 7.a), especially at 7 days of incubation (Figure 7.b). In comparison, cells cultured on coverslip and Titanium control surfaces exhibited vinculin diffusely distributed, with only few defined arrangements at the membrane border.

Enhanced expression of vinculin was observed in extended areas surrounding the nucleus, as well as in focal contact sites, especially in response to the laser nanostructured Ti surfaces after 7 days of culture, demonstrating excellent adhesion behavior of the cells to the surface of the laser processed samples (Figure 7.b). These results are correlated with statistically relevant data obtained in proliferation assay at 7 days of culture in direct contact with surface materials investigated (Figure 6), as compared with coverslip control or unprocessed Titanium surfaces.

This behavior could be correlated with an increased oxide layer on laser treated samples, since it was reported that a higher oxide thickness is beneficial for osteogenic activity and *in vivo* osseointegration [29] while a reduced oxide thickness was related to peri-implantitis, when combined with other factors [30].

Immunofluorescence microscopy imaging of the cytoskeleton has shown that all the Ti surfaces promote hMSCs adhesion at both time-points. We have found that picosecond laser nanostructuring of Ti surfaces is able to modulate hMSCs morphology to promote a better cell growth and adhesion after 7 days of culture in direct contact with the

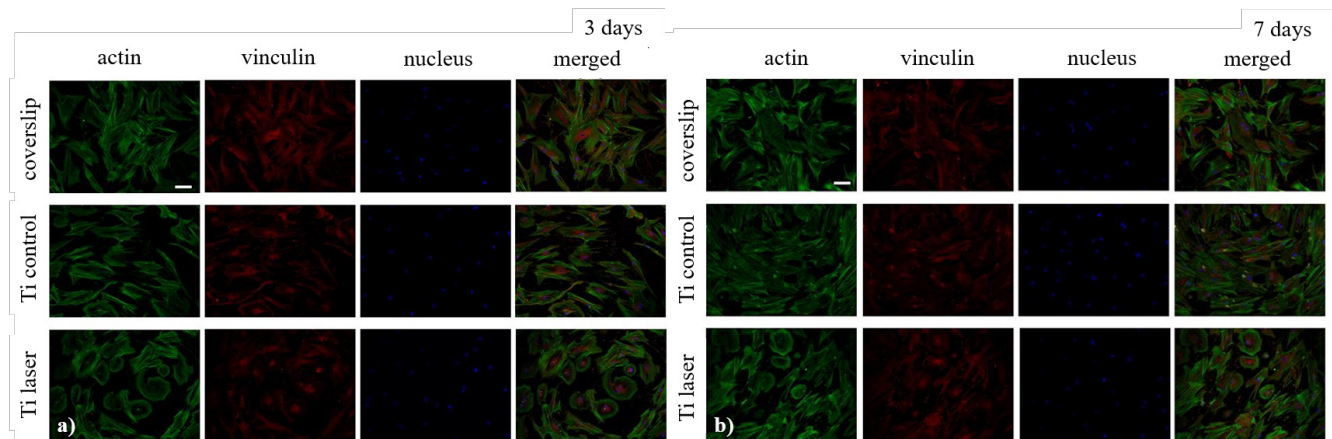
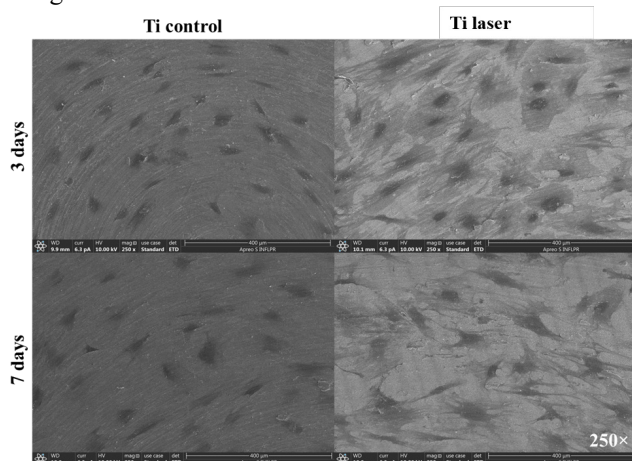


Fig. 7 Fluorescence microscopy images of hMSCs in direct contact with coverslip, Ti control and Ti laser processed at 3 days (a) and at 7 days (b) after cell seeding. Cytoskeleton proteins visualization: actin (green), vinculin (red) and nucleus (Hoechst-blue) using a 10× objective. Scale bar is 100 μm in all images.

surface as compared to control samples (either coverslip or unprocessed Ti surface) (Figure 7).

Scanning electron microscopy analyses revealed a better distribution of hMSCs cells on laser processed samples at both time intervals. Although hMSC cells exhibit a more rounded shape, the cells have a uniform pattern of spreading and are more elongated on laser processed surfaces (Figure 8). Actin and vinculin organization in response to different analyzed surfaces correlates with the cell attachment, spreading and morphology observed with SEM investigations.



**Fig. 8** SEM images of hMSCs grown on Ti control and laser processed samples at 3 days and 7 days after cell seeding. Magnification is 250 $\times$  in all images.

As perspectives, it would be very challenging to predict cells morphology change with LIPSS orientation. It is known that cell orientation is cell-type dependent and is significantly evident when the periodicity of LIPSS is above a critical value. The preferential cell orientation is also influenced by LIPSS uniformity on surface. It was shown that human embryonic kidney (HEK-293) and Chinese hamster ovary (CHO-K1) cells align along the direction of the ripples for periods above 340 nm and rat skeletal myoblast aligns on the ripples with periodicities over 430 nm, while human myoblasts only align for periodicities above 270 nm on polystyrene LIPSS (31). In case of mesenchymal stem cells (C3H10 T1/2 murine) cultivated on LIPSS obtained at TiAlV substrate surface, they were shown to be more sensitive to nanoscale LIPSS when these are generated on substrate micro-grooves with sizes close to the cell size and deeper than 5 $\mu$ m (32). On the other hand, in another study, when hMSCs were cultured on modified TiAlV substrates in osteogenic medium, they demonstrated osteoblastic commitment, while LIPSS textured surfaces with periodicities about 700 nm enhanced matrix mineralization and bone-like nodule formation as compared with polished surfaces (33). It would be then of interest to combine surface microstructuring with various nanoscale LIPSS in order to tailor cell behavior for specific applications, in particular dental abutments.

#### 4. Conclusion

High-repetition rate picosecond laser processing was proposed for Titanium surface nanostructuring. Laser-induced periodic surface structures (LIPSS) are generated on large-scale areas, with surface morphologic features

tailored by the applied irradiation dose. The surface composition was also modified by laser irradiation. It was found that oxygen concentration increases with the applied laser dose, revealing the formation of a thicker oxide layers. Ti surfaces processed by picosecond laser nanostructuring were further found to modulate human mesenchymal stem cells viability and proliferation through morphological modifications and promote a better cells growth and adhesion as compared with control after 7 days of culture.

#### Acknowledgments

This work was supported by POC 361 project (Funcționizarea suprafeței transmucozale la bonturile protetice pe implanturile dentare în scopul sigilării spațiului perimplanta - SMIS 122040) and by Romanian Ministry of Education and Research, under Romanian National Nucleu Programme LAPLAS VII.

#### References

- [1] R. Depprich, M. Ommerborn, H. Zipprich, C. Naujoks, J. Handschel, H.-P. Wiesmann, N.R. Kübler, U. Meyer: *Head Face Med.*, 4, (2008) 29.
- [2] P. Rezvanian, R. Daza, P. A. López, M. Ramos, D. González-Nieto, M. Elices, G.V. Guinea, J. Pérez-Rigueiro: *Sci. Rep.*, 8, (2018) 3337.
- [3] A. Civantos, E. Martínez-Campos, V. Ramos, C. Elvira, A. Gallardo, A. Abarrategi: *ACS Biomater. Sci. Eng.*, 3, (2017) 1245.
- [4] K. Anselme: *Biomaterials*, 21, (2000) 667.
- [5] K. Anselme, P. Linez, M. Bigerelle, D. Le Maguer, A. Le Maguer, P. Hardouin, H.F. Hildebrand, A. Iost, J.M. Leroy: *Biomaterials*, 21, (2000) 1567.
- [6] N. Marín-Pareja, M. Cantini, C. González-García, E. Salvagni, M. Salmerón-Sánchez, M.-P. Ginebra: *ACS Appl. Mater. Interfaces*, 7, (2015) 20667.
- [7] A.L. Palkowitz, T. Tuna, S. Bishti, F. Böke, N. Steinke, G. Müller-Newen, S. Wolfart, H. Fischer: *Adv. Healthcare Mater.*, 10, (2021) 2100132.
- [8] A. Kurup, P. Dhattrak, N. Khasnis: *Materials Today: Proceedings*, 39, (2021) 84.
- [9] S. Li, J. Ni, X. Liu, X. Zhang, S. Yin, M. Rong, Z. Guo, L. Zhou: *J Biomed Mater Res Part B*, 100B, (2012) 1587.
- [10] L.-C. Zhang, L.-Y. Chen, L. Wang: *Advanced Engineering Materials*, 22, (2020) 1901258.
- [11] X. Liu, P.K. Chu, C. Ding: *Materials Science and Engineering: R*, 47, (2004) 49.
- [12] E. Axente, L.E. Sima, F. Sima: *Coatings*, 10, (2020) 463.
- [13] S. Antony, T.R. Anju, B. Thomas: "Nature-Inspired Biomimetic Polymeric Materials and Their Applications" In: "Handbook of Biopolymers" ed. by S. Thomas, A. AR, C. J. Chirayil, B. Thomas, (Springer, Singapore 2022) p. 1.
- [14] F. Sima, P. Davidson, E. Pauthe, L.E. Sima, O. Gallet, I.N. Mihailescu, K. Anselme: *Acta Biomaterialia*, 7, (2011) 3780.
- [15] F.J.C. Braga, R.F.C. Marques, E. de A. Filho, A.C. Guastaldi: *Applied Surface Science*, 253, (2007) 9203.
- [16] E. Stratakis, J. Bonse, J. Heitz, J. Siegel, G.D. Tsibidis, E. Skoulas, A. Papadopoulos, A. Mimidis, A.-C. Joel, P. Comanns, J. Krüger, C. Florian, Y.

- Fuentes-Edfuf, J. Solis, W. Baumgartner, *Materials Science & Engineering R*, 141, (2020) 100562.
- [17] J. Bonse, J. Kruger, S. Hohm, A. Rosenfeld: *J. Laser Appl.*, 24, (2012) 042006.
- [18] G.D. Tsibidis, M. Barberoglou, P.A. Loukakos, E. Stratakis, C. Fotakis: *Phys. Rev. B* 86, (2012) 115316.
- [19] A. Rudenko and J.-P. Colombier: „How Light Drives Material Periodic Patterns Down to the Nanoscale”. In „Ultrafast Laser Nanostructuring”, eds. R. Stoian, J. Bonse, (Springer Nature Switzerland AG, 2023) p. 209.
- [20] J. Bonse, S.V. Kirner, J. Krüger: “Laser-Induced Periodic Surface Structures (LIPSS)”. In “Handbook of Laser Micro- and Nano-Engineering”, ed. K. Sugiooka, (Springer International Publishing: New York, NY, USA, 2021) p. 1.
- [21] J. Geng, L. Xu, W. Yan, L. Shi, M. Qiu: *Nature Communications*, 14, (2023) 565.
- [22] D. Cereška, A. Žemaitis, G. Kontenis, G. Nemickas, L. Jonušauskas: *Materials*, 15, (2022) 2141.
- [23] R.Y. Siddiquie, A. Gaddam, A. Agrawal, S.S. Dimov, S.S. Joshi: *Langmuir*, 36, (2020) 5349.
- [24] L. Sotelo, T. Fontanot, S. Vig, P. Herre, P. Yousefi, M.H. Fernandes, G. Sarau, G. Leuchs, S. Christiansen: *Adv. Mater. Technol.*, 8, (2023) 2201802.
- [25] G. Negroiu, R.M. Piticescu, G.C. Chitanu, I.N. Mihailescu, L. Zdrentu, M. Miroiu: *J. Mater. Sci.*, 19, (2008) 1537.
- [26] C. Florian, R. Wonneberger, A. Undisz, S.V. Kirner, K. Wasmuth, D. Spaltmann, J. Krüger, J. Bonse: *Applied Physics A*, 126, (2020) 1.
- [27] P. Fosodeder, W. Baumgartner, C. Steinwender, A.W. Hassel, C. Florian, J. Bonse, J. Heitz: *Adv. Opt. Techn.* 9, (2020) 113.
- [28] F. Xia, L. Jiao, D. Wu, S. Li, K. Zhang, W. Kong, M. Yun, Q. Liu, X. Zhang: *Optical Materials Express*, 9, (2019) 4097.
- [29] G. Wang, J. Li, K. Lv, W. Zhang, X. Ding, G.-Z. Yang, X. Liu, X. Jiang: *Sci Rep*, 6, (2016) 31769.
- [30] J. Mouhyi, D.M. Dohan Ehrenfest, T. Albrektsson: *Clinical Implant Dentistry and Related Research*, 14, (2012) 170.
- [31] E. Rebollar, I. Frischauf, M. Olbrich, T. Peterbauer, S. Hering, J. Preiner, P. Hinterdorfer, C. Romanin, J. Heitz: *Biomaterials*, 29, (2008) 1796.
- [32] O. Raimbault, S. Benayoun, K. Anselme, C. Mauclair, T. Bourgade, A.-M. Kietzig, P.-L. Girard-Lauriault, S. Valette, C. Donnet: *Materials Science and Engineering: C*, 69, (2016) 311.
- [33] A. Cunha, O.F. Zouani, L. Plawinski, A.M. Botelho do Rego, A. Almeida, R. Vilar, M.-C. Durrieu: *Nanomedicine*, 10, (2015) 725.

(Received: June 14, 2023, Accepted: September 30, 2023)